Revisiting 2π phase slip suppression in topological Josephson junctions

Rosa Rodríguez-Mota,[1] Smitha Vishveshwara,[2] and T. Pereg-Barnea[1,3]

[1]*Department of Physics and the Centre for Physics of Materials, McGill University, Montreal, Quebec, Canada H3A 2T8*
[2]*Department of Physics, University of Illinois at Urbana-Champaign, Urbana, Illinois 61801-3080, USA*
[3]*Department of Condensed Matter Physics, Weizmann Institute of Science, Rehovot 76100, Israel*

Current state-of-the-art devices for detecting and manipulating Majorana fermions commonly consist of networks of Majorana wires and tunnel junctions. We study a key ingredient of these networks—a topological Josephson junction with charging energy—and we pinpoint crucial features for device implementation. The phase-dependent tunneling term contains both the usual 2π-periodic Josephson term and a 4π-periodic Majorana tunneling term representing the coupling between Majoranas on both sides of the junction. In nontopological junctions when the charging energy is small compared to the Josephson tunneling scale, the low-energy physics is described by 2π phase slips. By contrast, in a topological junction, due to the 4π periodicity of the tunneling term, it is usually expected that only 4π phase slips are possible while 2π phase slips are suppressed. However, we find that if the ratio between the strengths of the Majorana assisted tunneling and the Josephson tunneling is small, as is likely to be the case for many setups, 2π phase slips occur and may even dominate the low-energy physics. In this limit, one can view the 4π phase slips as a pair of 2π phase slips with arbitrarily large separation. We provide an effective description of the system in terms of 2π and 4π phase slips valid for all values of the tunneling ratio. Comparing the spectrum of the effective models with numerical simulations, we determine the crossover between the 4π phase slip regime to the 2π phase slip dominated regime. We also discuss the role of the charging energy as well as the implications of our results on the dissipative phase transitions expected in such a system.

I. INTRODUCTION

In recent years, extensive scientific efforts have been invested to understand, realize, and manipulate topological states in condensed matter [1,2]. Particularly, topological superconducting wires [3,4], which are constructed using systems with strong spin-orbit coupling, induced Cooper pairing, and a Zeeman field, have gathered much attention [5]. Interest in these Majorana wires is motivated by the possibility of using the non-Abelian nature of Majorana modes for quantum computation schemes [6,7], and it is sustained by encouraging experimental results [8–16]. Hence, networks of Majorana wires have been proposed as tools to manipulate Majorana modes for quantum information purposes [17–22] or to create more exotic matter [23,24]. In this work, we study a phenomenon commonly relevant to this type of network, namely charge-induced quantum fluctuations in topological Josephson junctions.

In a superconductor, the charge is conjugate to the order parameter phase, and charging effects induce quantum phase fluctuations [25,26]. In a nontopological Josephson junction, tunneling processes are known as phase slips and are essentially 2π jumps in the phase difference between the superconductors. The delocalization of the phase induced by these fluctuations can be prevented by dissipation. As a result, Josephson junctions present a dissipative phase transition [27,28]. In a topological junction, which is composed of two topological superconductors, there are Majorana modes at both edges of the junction. The presence of these modes leads

to coherent single-particle tunneling between the superconductors, commonly referred to as the 4π periodic Josephson effect [3,4,7,29–32]. The change of periodicity in the overall tunneling current suppresses 2π phase slips in topological Josephson junctions [33]. Both the 2π phase slip suppression [33–35] and its effects on the dissipative phase transition [35] have been proposed as a probe for topological superconductivity. Most studies of 2π phase slip suppression focus on having a sufficiently strong single-particle tunneling [33–35]. This is despite the fact that the single-particle tunneling may be a small component of the overall tunneling current, as is the case for 3D topological insulator-based Josephson junctions [36,37]. As a result, there are currently no studies that describe the 2π phase slip suppression throughout the transition from a nontopological to a topological junction. Our work extends the existing literature and provides (a) a semiclassical description of 4π phase slips as coupled 2π phase slips, and (b) the relevant regimes for bound and unbound pairs of phase slips.

In this work, we develop a theory for the effect of charging-induced phase fluctuations in the low-energy spectrum of a topological Josephson junction, valid for any ratio of the single particle and the Cooper pair tunneling. Our results show that a description of the low-energy physics of the topological junction in terms of 4π phase slips alone is insufficient when the strength of the 4π periodic tunneling is too small. In the presence of both 2π and 4π periodic components of the tunneling current, the potential energy of the junction as a function of the phase difference between the superconductors,
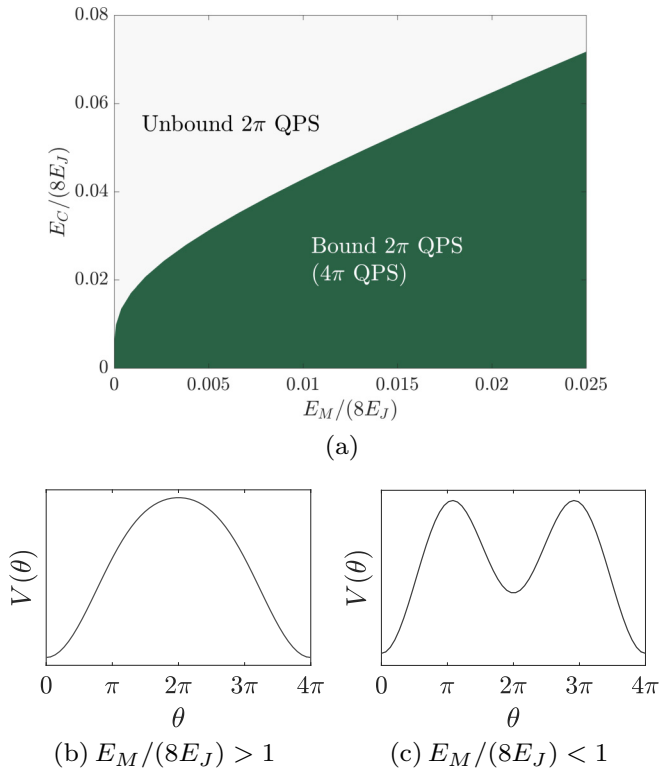
(a)

(b) $E_M/(8E_J) > 1$

(c) $E_M/(8E_J) < 1$

FIG. 1. Depending on the relative strength between the single particle (set by E_M) and the pair tunneling (set by E_J), the potential of the topological Josephson junction may be minimized when (b) the phase difference across the junction is an integer multiple of 4π only, or (c) the phase difference across the junction is any integer multiple of 2π. In (c) the minima at odd 2π are local minima. (a) In (c), the strength of phase fluctuations (set by the charging energy E_C) determines whether oscillations around the local minima contribute to the ground state (unbound 2π QPS) or not (4π QPS). The crossover is found numerically by evaluating the relative accuracy of the 4π and 2π phase slip scenarios.

θ, may have one or two minima in $[0, 4\pi)$ [see Figs. 1(b) and 1(c)]. If only one minimum exists, the description in terms of 4π phase slips is valid for small phase fluctuations. In the presence of two minima, this description may break down even for small phase fluctuations if they are relatively large compared to the strength of the 4π periodic tunneling. In this case, a description of the junction in terms of unbound 2π phase slips is more appropriate. This is shown in Fig. 1(a), where E_J and E_M correspond to the energy scale of the 2π and 4π periodic tunneling, respectively, and E_C to the strength of the phase fluctuations. The junction potential has only one minimum for $E_M > 8E_J$ and two otherwise.

We treat the appearance of phase slips in the topological Josephson junction in two ways. First, we calculate the phase slip probability using a semiclassical method where we calculate a path integral between a state with $\theta = 0$ in the distant past and $\theta = 4\pi$ in the distant future describing the phase slip process. We calculate the phase slip probability up to Gaussian fluctuations around this 4π instanton. While the phase slip probabilities for the case of nontopological junctions are well-known, we use the double-sine-Gordon formalism to derive

them for the case of a topological junction. In the small Majorana tunneling regime, we assume dominance of 2π phase slips and calculate their probability using a method for asymmetric barriers [38]. Secondly, we solve the problem numerically in a truncated Hilbert space. The numerics give us the ground-state energy of the junction as a function of a tuning parameter, which we can compare with the spectrum expected for the 2π and 4π phase slip scenarios. This gives us a regime of validity for either scenario and therefore a crossover between the two behaviors, as depicted in Fig. 1(a).

This paper is organized as follows. In Sec. II, we give a brief review of the effects of charging-induced phase fluctuations in Josephson junctions. The review is followed by a qualitative discussion of the effects of phase fluctuations for different regimes of a topological Josephson junction in Sec. III. The main results are stated in Sec. IV, where we introduce low-energy effective models of topological Josephson junctions. In Sec. VI we discuss the implications of our results on the dissipative phase transition. Our conclusions are stated in Sec. VII.

II. REVIEW OF THE EFFECTS OF QUANTUM PHASE SLIPS IN JOSEPHSON JUNCTIONS

We begin with a quick review of the effects of small phase fluctuations in a nontopological junction. The junction consists of a weak link between two superconductors with a junction capacitance C described by the Hamiltonian

$$\hat{H} = E_C(\hat{n} - n_g)^2 - E_J \cos\hat{\theta}, \qquad (1)$$

where E_J is the Josephson energy associated with the tunneling of Cooper pairs between the two superconductors, $E_C = e^2/(2C)$ is the charging energy of the weak link, and n_g is the offset charge. The operator $\hat{n}$ measures the charge, and the operator $\hat{\theta}$ measures the phase difference between the superconductors. To simplify the comparison with the following sections, we measure $\hat{n}$ (and n_g) in units of the electron charge e, rather than in the more conventional units of $2e$. The commutation relation, $[\hat{\theta}, \hat{n}] = 2i$, therefore follows. Several examples of superconducting circuits, such as the ones used in the Cooper pair box [39,40], namely quantronium [41] and transmon [42] qubits, can be mapped to Eq. (1). In these circuits, n_g is tuned using gate voltages, while the ratio of E_J and E_C may be tuned using split junctions or by adding additional capacitances (see, e.g., Ref. [43]).

On the basis of phase eigenstates, the wave function $\Psi(\theta) = \langle\theta|\Psi\rangle$ describing the Josephson junction follows the equation

$$\left[E_C\left(-2i\frac{d}{d\theta} - n_g\right)^2 - E_J \cos\theta \right]\Psi(\theta) = E\Psi(\theta) \qquad (2a)$$

respecting the boundary condition

$$\Psi(\theta + 2\pi) = \Psi(\theta). \qquad (2b)$$

The dependence of the system on the offset charge n_g can be transferred from Schrödinger's equation to the boundary

condition via $\Psi(\theta) \to e^{in_g\theta/2}\Psi(\theta)$, which results in

$$\left[E_C\left(-2i\frac{d}{d\theta}\right)^2 - E_J\cos\theta\right]\Psi(\theta) = E\Psi(\theta), \qquad (3a)$$

$$\Psi(\theta + 2\pi) = e^{i\pi n_g}\Psi(\theta). \qquad (3b)$$

The above equations can be solved using Mathieu functions. Nonetheless, expansions for different parameter regimes have been developed to provide more intuition. Since we are interested in studying phase fluctuations, we focus on the $E_C \ll E_J$ limit. This corresponds to the regime of interest of transmon qubits [42].

When $E_C \ll E_J$ the potential energy $-E_J\cos\theta$ dominates the energy of the system. Around the potential energy minima, at $\theta = 2\pi j$ with integer j, Eq. (3a) can be mapped onto a harmonic oscillator having frequency $\hbar\omega = \sqrt{8E_J E_C}$. The low energy levels of the Josephson junction, therefore, correspond to harmonic-oscillator levels. Deep inside the potential well, these harmonic oscillations do not depend on the boundary conditions given by Eq. (3b). To find the junction dependence on n_g, we need to account for quantum tunneling between the different potential minima.

Denoting the amplitude for quantum tunneling between the mth harmonic-oscillator level of one of the potential minima and its nearest neighbors by ν_m, it is possible to write an effective tight-binding Hamiltonian for the junction:

$$\hat{H} = \sum_{m=0}^{\infty}\sum_j [\epsilon_m a_{m,j}^\dagger a_{m,j} - \nu_m a_{m,j+1}^\dagger a_{m,j} + \text{H.c.}]. \qquad (4)$$

Here $a_{m,j}^\dagger$ is the creation operator for the mth level of a harmonic oscillator around $2\pi j$, and $\epsilon_m = \hbar\omega(m + 1/2)$ is the energy of the a level. The tight-binding Hamiltonian in Eq. (4) is diagonalized using the operators $a_{m,k} = \sum_j e^{-ikj}a_{m,j}$:

$$\hat{H} = \sum_m\sum_k (\epsilon_m - 2\nu_m\cos k)a_{m,k}^\dagger a_{m,k}. \qquad (5)$$

Comparing with Eq. (3b) leads to the identification $k = \pi n_g$, which allows us to conclude that for $E_C \ll E_J$ the dispersion of the mth level of the junction is given by

$$E_m(n_g) = \epsilon_m - 2\nu_m\cos(\pi n_g), \qquad (6)$$

which holds when $\nu_m \ll \hbar\omega$.

The tunneling amplitudes ν_m can be calculated using semi-classical methods. Here we briefly outline the calculation for the lowest energy level corresponding to the phase slip probability ν_0. We use the dilute instanton gas approximation in the path integral imaginary-time formalism (see, e.g., Ref. [44]). In this formalism, the amplitude to propagate from 0 to 2π during an imaginary-time interval of length $2L$ is written as a weighted sum over all the paths that start at 0 at time $\tau = -L$ and end at 2π at $\tau = L$:

$$(0, -L|2\pi, L) = \int[\mathcal{D}\theta]e^{-\frac{1}{\hbar}\int_{-L}^{L}\mathcal{L}[\theta(\tau)]d\tau}, \qquad (7)$$

where

$$\mathcal{L}(\theta) = \frac{\hbar^2(\partial_\tau\theta)^2}{16E_C} + E_J(1 - \cos\theta) \qquad (8)$$

is commonly known as the sine-Gordon Lagrangian, which is related to the Hamiltonian in Eq. (1) through a Legendre transform.

For $L \to \infty$ the classical solution is a 2π-kink, also referred to as an instanton. It is given by $\theta_{2\pi}^{\text{cl}}(\tau) = 4\arctan(e^{\omega(\tau - \tau_0)})$, where $\omega = \sqrt{E_J E_C}/\hbar$ coincides with the frequency of harmonic oscillations around the $2\pi j$ minima. Conversely, the model also has a classical solution with $\theta(-\infty) = 2\pi$ and $\theta(\infty) = 0$ known as an antikink. In the dilute instanton gas approximation, the path integration of Eq. (7) is done over combinations of kinks and antikinks and Gaussian fluctuations around them. Furthermore, it is assumed that the kinks and antikinks are separated enough (in imaginary time) that the interactions between them are negligible. This yields the result

$$\nu_0 = \sqrt{2(\hbar\omega)^3/(\pi E_C)}e^{-\hbar\omega/E_C}, \qquad (9)$$

where $\hbar^2\omega/E_C = \hbar\sqrt{8E_J/E_C}$ is the action of a 2π kink.

To test the validity of Eq. (9), we ask whether the gas of kinks and antikinks is in fact dilute. This can be done by comparing the width of the kinks, $2/\omega$, with the expected average separation among them, $\hbar/\nu_0$. The gas is dilute, and Eq. (9) is self-consistent, as long as $\nu_0 \ll \hbar\omega/2$, which is satisfied for $E_J \gg E_C$.

This formalism can be extended to calculate the n_g dependence of higher levels through the use of periodic instantons (see, e.g., Ref. [45]). The decision to focus on ν_0 was made for the sake of simplicity.

III. PHASE FLUCTUATIONS IN A TOPOLOGICAL JOSEPHSON JUNCTION

In a topological junction, the two superconductors coupled by the junction each present a Majorana mode close to the junction. We denote these by γ_1 and γ_2, and we ignore the other two Majorana modes, which are far from the junction. The coupling of these Majorana modes adds a 4π periodic term to the tunneling current [3,4,7,29–32]. The topological junction can then be modeled by the following Hamiltonian:

$$\hat{H} = E_C(\hat{n} - n_g)^2 - E_J\cos\hat{\theta} - i\gamma_1\gamma_2\frac{E_M}{2}\cos\frac{\hat{\theta}}{2}, \qquad (10)$$

where $i\gamma_1\gamma_2$ is the parity of the fermionic mode caused by the hybridization of the Majorana modes on both sides of the junction.

A physical realization of the above phenomenological model is possible using a Majorana Cooper pair box, such as the one studied in Ref. [46]. To achieve the desired phase-dominated limit, the Majorana Cooper pair box could be shunted by a larger capacitance, as is done in transmon qubits [42].

If the local parity is conserved, the operator $i\gamma_1\gamma_2$ in Eq. (10) can be substituted by either one of its two eigenvalues ± 1. Without loss of generality, from now on we assume $i\gamma_1\gamma_2 = 1$. As long as the local parity is conserved, our results do not rest on this assumption. As in the previous section, after a charge translation the wave function in phase basis follows

(a) $E_C = 0.001$
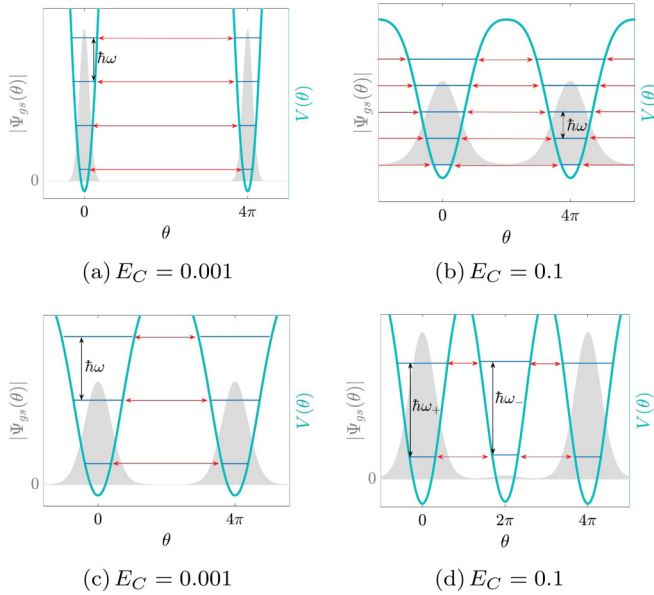
(b) $E_C = 0.1$

(c) $E_C = 0.001$

(d) $E_C = 0.1$

FIG. 2. Phase fluctuations in the single-minimum and double-minimum regimes of a topological Josephson junction. The first harmonic levels (blue lines) and the junction potential (green line) are shown for a junction with $E_M = 2 = 10E_J$ and (a) $E_C = 0.001$ and (b) $E_C = 0.1$, and a junction with $E_J = 1 = 50E_M$ and (c) $E_C = 0.001$ and (d) $E_C = 0.1$. The ground-state wave functions (amplitudes shown in gray) correspond to linear superpositions of harmonic oscillations around the potential minima. The tunneling processes that give rise to the n_g dispersion of each level are shown in red. In the double-minimum regime [(c) and (d)], increasing E_C can change the dominant tunneling processes. The ground-state wave function in (d) shows an additional (small) peak around 2π. Note that in panels (c) and (d), the 2π minimum is not degenerate with the 4π ones.

an n_g-independent Schrödinger's equation:

$$\left[E_C \left(-2i \frac{d}{d\theta} \right)^2 - E_J \cos\theta - \frac{E_M}{2} \cos\frac{\theta}{2} \right] \Psi = E\Psi \quad (11a)$$

and a boundary condition

$$\Psi(\theta + 4\pi) = e^{i2\pi n_g} \Psi(\theta). \quad (11b)$$

As in the nontopological case, when E_C is small compared to the tunneling E_J and E_M, the energy is dominated by the tunneling terms, which we refer to as "the potential." We therefore expect the ground-state wave function to be concentrated around the potential minima. In the topological Josephson junction, the competition between the pair and single-particle tunneling creates two different regimes depending on whether the junction potential has a single minimum or two minima for $0 \leqslant \theta < 4\pi$.

When $E_M/(8E_J) > 1$, the junction potential has a single minimum in the $[0, 4\pi)$ interval. Hence, the potential is minimized when $\theta = 4\pi m$, with m an integer, and all the minima are degenerate. The frequency of harmonic oscillations around these minima, obtained by expanding Eq. (11a) around these values, is $\hbar\omega = \sqrt{8E_J E_C + E_M E_C}$. This is exemplified in Fig. 2(a), where the first few harmonic-oscillator levels and the ground-state wave-function amplitude are shown for

$E_M = 2 = 10E_J$ and $E_C = 0.001$. The junction potential and the tunneling processes between the degenerate levels are also shown in Fig. 2(a). As E_C increases, the spacing between the levels and tunneling amplitude increases and the harmonic wave functions widen, as shown in Fig. 2(b) for $E_M = 2 = 10E_J$ and $E_C = 0.1$. However, the tunneling processes that give rise to the n_g dispersion remain unchanged by the increase of E_C. In this regime, the topological junction behaves qualitatively similar to the nontopological junction from the previous section with half the n_g periodicity and 4π phase slips taking the role of 2π phase slips.

On the other hand, if $E_M/(8E_J) < 1$, the junction potential has two minima in the $[0, 4\pi)$ interval. Hence, the potential has two kinds of minima with two different frequencies for harmonic oscillations around them: $\theta = 4\pi m$ with frequency $\hbar\omega_+ = \sqrt{8E_J E_C + E_M E_C}$, and $\theta = 4\pi m + 2\pi$ with frequency $\hbar\omega_- = \sqrt{8E_J E_C - E_M E_C}$. In addition to the effects discussed in the previous paragraph, changing E_C may also change the tunneling processes that contribute to each energy level. This is shown in Figs. 2(c) and 2(d). The ground-state wave function in Fig. 2(c) is peaked around 0 and 4π, whereas the ground-state wave function in Fig. 2(d) shows additional contributions from oscillations around 2π.

IV. EFFECTIVE MODELS

In this section, we will discuss two different effective models for the junction ground state: one in which only oscillations between $4\pi m$ minima contribute and one in which oscillations around all $2\pi m$ minima contribute to the ground state. We calculate the effective hopping parameters of each model and discuss their regions of validity.

A. 4π QPS model

We can write an effective Hamiltonian for the ground state of the junction as a combination of harmonic oscillations around $4\pi j$ plus hopping between such minima:

$$\hat{H} = \sum_j \left(\frac{\hbar\omega}{2} a_j^\dagger a_j - v_{4\pi} a_{j+1}^\dagger a_j + \text{H.c.} \right), \quad (12)$$

where ω the frequency of harmonic oscillations around the minima at $4\pi j$ and is given by $\hbar\omega = \sqrt{8E_J E_C + E_M E_C}$. Accounting for the boundary condition, Eq. (11b), results in the following ground-state energy dispersion:

$$E_{gs}(n_g) = \frac{\hbar\omega}{2} - 2v_{4\pi} \cos(2\pi n_g). \quad (13)$$

This model gives an effective description of the system in the single-minimum regime and in the double-minimum regime for small enough E_C (see Fig. 2).

The tunneling amplitude $v_{4\pi}$ can be calculated following the procedure outlined in Sec. II. The imaginary-time Lagrangian of the topological junction,

$$\mathcal{L}(\theta) = \frac{\hbar^2(\partial_\tau\theta)^2}{16E_C} + E_J(1 - \cos\theta) + \frac{E_M}{2}\left(1 - \cos\frac{\theta}{2}\right), \quad (14)$$

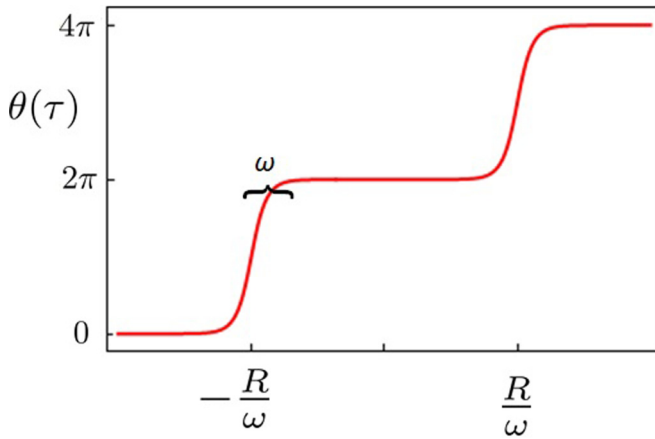is known as the double sine-Gordon Lagrangian, and its semiclassical dynamics have been widely studied [47].

FIG. 3. A 4π instanton is made of two 2π instantons of width ω separated by an imaginary time of $2R/\omega$.

Interestingly, as shown in Fig. 3, the 4π kink in the DSG model can be written as a sum of two 2π SG kinks:

$$\theta_{4\pi}^{cl} = 4 \arctan e^{\omega(\tau-\tau_0)-R} + 4 \arctan e^{\omega(\tau-\tau_0)+R}. \quad (15a)$$

The imaginary-time separation of the two 2π kinks, $2R/\omega$, is set by the ratio of E_M and $8E_J$ as R is given by

$$R = \operatorname{arccosh}\left(\sqrt{1 + \frac{8E_J}{E_M}}\right). \quad (15b)$$

The 4π DSG kink is depicted in Fig. 3. The width of the kinks is controlled by the Josephson tunneling and the capacitance energy through $\omega = \sqrt{E_J E_C}/\hbar$, and the separation between kinks is controlled by the ratio of E_M and E_J through $2R/\omega$. When $E_M \to 0$, the separation between the two 2π kinks diverges ($R \to \infty$), meaning that the 4π kinks effectively decouple into two separate 2π kinks as the DSG Lagrangian reduces to the SG Lagrangian.

Using the dilute instanton gas approximation, as before, we find

$$\nu_{4\pi} = \sqrt{\frac{8(\hbar\omega)^5}{\pi E_M E_C^2}} \exp\left[-\frac{\hbar\omega}{E_C} \times f\left(\frac{E_M}{8E_J}\right)\right], \quad (16a)$$

where

$$f(x) = 2 + \frac{2x}{\sqrt{1+x}} \coth^{-1}(\sqrt{1+x}) \quad (16b)$$

is an increasing function with $f(0) = 2$ and $f(\infty) = 4$. With the appropriate modifications, this result is in agreement with the result found by Ref. [48] in the context of statistical mechanics. A more detailed derivation of how Eq. (16) is obtained is shown in Appendix A 1.

When $E_M \to 0$, $\nu_{4\pi}$ presents a square-root divergence, i.e., $\nu_{4\pi} \sim 1/\sqrt{E_M}$. This divergence has two physical interpretations. First, it is indicative of a resonance in tunneling [49] when $E_M \to 0$. In our context, it is a sign that the validity of the model breaks down in this limit. Secondly, this divergence is indicative of the restoration of a symmetry. In this case, the symmetry that is restored is the 2π translation symmetry, i.e., the decoupling of the two 2π kinks.

The restoration of the 2π translation symmetry for $E_M \to 0$ diminishes the range of the validity of the calculated expression for $\nu_{4\pi}$. This can be seen by noting that the dilute instanton gas approximation breaks down when $E_M \to 0$: the width of the 4π kinks $(2 + 2R)/\omega$ diverges as $-\log E_M$, whereas the average separation between the kinks $\hbar/\nu_{4\pi}$ goes to zero as $\sqrt{E_M}$. The assumption that the width of the 4π kinks is much smaller than the average separation between the kinks fails for $E_M \to 0$. We address this problem in the next subsection.

Emergent translational mode correction

To derive a semiclassical expression whose validity extends to smaller E_M/E_J ratios, we account for a higher order of fluctuations in the direction of the emergent translational mode [50,51]. Since the emergent translational mode is related to the decoupling of the two kinks, this is roughly equivalent to letting the distance between the two kinks fluctuate around its equilibrium value, $2R/\omega$.

The result of Ref. [51] can be written in terms of R as

$$\nu_{4\pi} = \frac{4F(R)(\hbar\omega)^2}{\pi E_C} \mathcal{I}\left(R, \frac{\hbar\omega}{E_C}\right), \quad (17a)$$

where $F(R)$ is a numerical factor bound by $\sqrt{2/5} \leqslant F(R) \leqslant 1$ and is given by

$$F(R) = \frac{\sqrt{\cosh 2R - R\tanh R - 3R\coth R + 2}}{\sinh R \sqrt{2 - 8R^2 \operatorname{csch}^2 2R}} \quad (17b)$$

and

$$\mathcal{I}(R, \alpha) = \int_0^\infty dr \sqrt{1 - 4r^2 \operatorname{csch}^2(2r)} e^{-\alpha S_R(r)} \quad (17c)$$

with

$$S_R(r) = 1 + \frac{\tanh^2 R}{\tanh^2 r} + 2r\left(\frac{1}{\sinh 2r} + \frac{\coth r}{\cosh^2 R}\right.$$
$$\left. - \frac{\tanh^2 R \coth r}{2\sinh^2 r}\right). \quad (17d)$$

In the above expressions, $2r/\omega$ corresponds to the fluctuating distance between the two kinks, and $S_R(r)$ is an r-dependent effective action, which is minimized at $r = R$. For more details on how this expression is obtained, see Appendix A 2 and Ref. [51].

To the best of our knowledge, a closed-form expression for $\mathcal{I}(R, \alpha)$ does not exist. Nonetheless, we can find approximate expressions for $\mathcal{I}(R, \alpha)$ for small and large R. When R is large, the integral is dominated by the linear large-r behavior of $S_R(r)$. In Appendix B 2, we find that for $16\alpha^2 \ll e^{2R}$,

$$\mathcal{I}(R, \alpha) \approx \frac{\cosh^2(R)e^{-\alpha(\tanh^2(R)+1)}}{2\alpha}. \quad (18)$$

This leads to $\nu_{4\pi} \approx \nu_{4\pi}^{lr}$ with

$$\nu_{4\pi}^{lr} = \frac{f_2\left(\frac{E_M}{8E_J}\right)(\hbar\omega)^3}{\pi E_C E_M} \exp\left[-\frac{\hbar\omega}{E_C} \times f_1\left(\frac{E_M}{8E_J}\right)\right] \quad (19)$$

when $E_M/(8E_J) \ll 0.25 E_C^2/(\hbar\omega)^2$. In the above equation, $f_1(x)$ and $f_2(x)$ are order 1 numerical factors that decrease

with x; their exact form can be found in Appendix B 2. Note that according to the above calculations, $\nu_{4\pi}$ diverges for $E_M \to 0$ as $1/E_M$.

For small R, the greatest contribution to $\mathcal{I}(R, \alpha)$ comes from the r values around R. A saddle-point approximation of the integral $\mathcal{I}(R, \alpha)$ results in

$$\mathcal{I}(R, \alpha) \approx \sqrt{\frac{\pi}{2\alpha}} \frac{\cosh R}{F(R)} e^{-\alpha S_R(R)}. \tag{20}$$

This is a good approximation to $\mathcal{I}(R, \alpha)$ if $e^{2R} \ll 16\alpha$ (see Appendix A 2). Substituting this in Eq. (17a) gives the expression for $\nu_{4\pi}$ obtained without including corrections due to the emergent translational mode, i.e., Eq. (16). Hence, Eq. (16) is valid when $E_M/(8E_J) \gg E_C/(4\hbar\omega)$.

We thus find that whether the distance between the two 2π phase slips R is fixed depends on how $E_M/(8E_J)$ compares with $E_C/(4\hbar\omega)$. Since

$$\frac{E_C}{4\hbar\omega} = \frac{E_C}{4\sqrt{8E_J E_C}} - \frac{E_C E_M}{64 E_J \sqrt{8E_J E_C}} + O(E_M^2), \tag{21}$$

$E_M/(8E_J) \sim E_C/(4\hbar\omega)$ when $E_M \sim (8E_J E_C)/(E_C/2 + \sqrt{8E_J E_C})$. Roughly, the distance between the two 2π phase slips R will be fixed when E_M is greater than this value, and it will fluctuate when it is smaller.

B. Coupled 2π QPS model

If the junction parameters are such that there are additional (local) minima at $2\pi m$ with m odd, and oscillations around those minima contribute to the ground state [see, e.g., Fig. 2(d)], we can describe it by the following effective Hamiltonian:

$$\hat{H} = \sum_j (\epsilon_j a_j^\dagger a_j - \nu_{2\pi} a_{j+1}^\dagger a_j - \nu_{2\pi} a_j^\dagger a_{j+1}), \tag{22}$$

where $\nu_{2\pi}$ corresponds to the tunneling amplitude between potential minima separated by 2π. The energies ϵ_n are given by

$$\epsilon_{2n} = \epsilon_e = \frac{\hbar\omega_+}{2},$$
$$\epsilon_{2n+1} = \epsilon_o = E_M + \frac{\hbar\omega_-}{2}, \tag{23}$$
$$\hbar\omega_\pm = \sqrt{8E_J E_C \pm E_M E_C}.$$

The dispersion of Eq. (22) is

$$E_\pm(n_g) = \frac{1}{2}(\epsilon_o + \epsilon_e)$$
$$\pm \frac{1}{2}\sqrt{(\epsilon_o - \epsilon_e)^2 + 8\nu_{2\pi}^2[1 + \cos(2\pi n_g)]}. \tag{24}$$

The hopping $\nu_{2\pi}$ can be calculated using the formula proposed by Ref. [38] for the tunneling through an asymmetric potential. Without loss of generality, we can focus on calculating the amplitude for tunneling between 0 and 2π. The minimum at 0 and the minimum at 2π are separated by a barrier that is largest at θ_{max}. Following Ref. [38], we define two potentials symmetric around θ_{max}, $V_L(\theta)$ and $V_R(\theta)$, such that $V_L(\theta)$ [$V_R(\theta)$] is equal to the junction potential for $0 < \theta < \theta_{max}$ ($\theta_{max} < \theta < 2\pi$). Then $\nu_{2\pi}$ can be written as

$$\nu_{2\pi} = A\sqrt{\nu_L \nu_R}, \tag{25}$$

where ν_s, $s = L, R$, is the probability for tunneling from 0 to 2π through the potential V_s and

$$A = \frac{1}{2}\left[\left(\frac{V_{max} - \epsilon_e}{V_{max} - \epsilon_o}\right)^{1/4} + \left(\frac{V_{max} - \epsilon_o}{V_{max} - \epsilon_e}\right)^{1/4}\right]^{1/2}, \tag{26}$$

with $V_{max} = V(\theta_{max})$. The above expression for $\nu_{2\pi}$ clearly breaks down when $\epsilon_o \geqslant V_{max}$; at that point, the zero-point motion of the shallow minimum becomes larger than the potential barrier. The approximations leading to the above expression for $\nu_{2\pi}$ start failing before this point.

For our model of a topological Josephson junction, θ_{max} and V_{max} are given by

$$\theta_{max} = 4\arctan(\omega_+/\omega_-),$$
$$V_{max} = 2E_J[E_M/(8E_J) + 1]^2, \tag{27}$$

and the θ_{max}-symmetric potentials V_L and V_R are well approximated by

$$V_L(\theta) \approx E_J\left(1 + \frac{E_M}{8E_J}\right)^2\left[1 - \cos\left(\frac{\pi\theta}{\theta_{max}}\right)\right],$$
$$V_R(\theta) \approx E_M + E_J\left(1 - \frac{E_M}{8E_J}\right)^2\left[1 - \cos\left(\frac{\pi(\theta - 2\pi)}{\theta_{max} - 2\pi}\right)\right], \tag{28}$$

which leads to the following tunneling amplitudes:

$$\nu_s = \frac{4}{\sqrt{P_s\pi}}\left(8E_s^3 E_C\right)^{1/4} e^{-P_s\sqrt{\frac{8E_s}{E_C}}} \tag{29}$$

with $P_L = \theta_{max}/\pi = 2 - P_R$, $E_L = E_J[1 + E_M/(8E_J)]^2$, and $E_R = E_J[1 - E_M/(8E_J)]^2$. P_s and E_s are, respectively, the period and amplitude of the potential V_s for $s = L, R$.

For $E_M \to 0$, the dispersion in Eq. (24) becomes

$$E_\pm(n_g) \to \frac{\hbar\omega}{2} \pm |2\nu_0\cos(\pi n_g)|. \tag{30}$$

This is the expected result for the $E_M \to 0$ limit, as it corresponds to the breaking of the symmetry between the minima at even and odd multiples of 2π "folding" the n_g-Brillouin zone.

We also note that for $\nu_{2\pi} \ll |\epsilon_o - \epsilon_e|$, the lowest of the two bands becomes

$$E_-(n_g) \approx \epsilon_e - \frac{2\nu_{2\pi}^2}{|\epsilon_o - \epsilon_e|} - \frac{2\nu_{2\pi}^2}{|\epsilon_o - \epsilon_e|}\cos(2\pi n_g). \tag{31}$$

This dispersion would be equivalent to the dispersion found for the 4π phase slip model (13) if $\nu_{2\pi}^2/|\epsilon_o - \epsilon_e| \to \nu_{4\pi}$. As shown in Fig. 4, we find that $\nu_{2\pi}^2/|\epsilon_o - \epsilon_e| \approx \nu_{4\pi}^{lr}$. This allows us to interpret $\nu_{4\pi}^{lr}$ as arising from coupled but not confined 2π phase slips. From this we conclude that the 2π phase slips become bound when $\nu_{2\pi} \ll |\epsilon_o - \epsilon_e|$. To provide a rough approximation for when the 2π phase slips are bound, we consider that

$$\nu_{2\pi} = \nu_0 + O(E_M^2) \quad \text{and}$$

$$|\epsilon_o - \epsilon_e| = E_M\left(1 - \frac{1}{2}\sqrt{\frac{E_C}{8E_J}}\right) + O(E_M^3) \tag{32}$$

so $\nu_{2\pi} \sim |\epsilon_o - \epsilon_e|$ when $E_M \sim \nu_0/(1 - \frac{1}{2}\sqrt{\frac{E_C}{8E_J}})$. The 2π phase slips bound for $E_M > \nu_0/(1 - \frac{1}{2}\sqrt{\frac{E_C}{8E_J}})$.
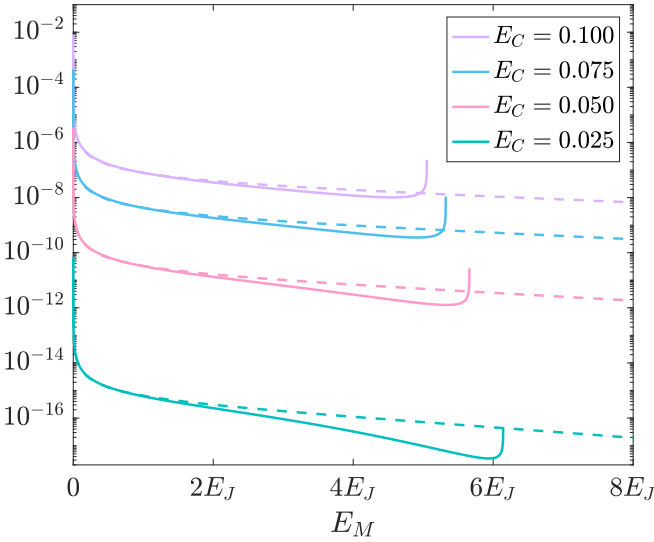
FIG. 4. Comparison of $\nu_{2\pi}^2/|\epsilon_o - \epsilon_e|$ (solid line) and $\nu_{4\pi}^{lr}$ (dashed line) for $E_J = 1$. The $\nu_{2\pi}^2/|\epsilon_o - \epsilon_e|$ lines stop when the potential barrier is smaller than the zero-point motion energy for oscillations around the shallow minima ϵ_o.

C. Validity of the effective models

The image that emerges from the results in this section and the previous energetic considerations is as follows. The 4π tunneling—whose strength is set by E_M—acts as a binding potential between pairs of 2π phase slips. We find three relevant regimes:

(i) *Unbound 2π phase slips.* For $0 < E_M < \nu_0/(1 - \frac{1}{2}\sqrt{\frac{E_C}{8E_J}})$, the 2π phase slips couple to each other but the 4π tunneling is not strong enough to bind them.

(ii) *Bound 2π phase slips with fluctuating* **R**. For $\nu_0/(1 - \frac{1}{2}\sqrt{\frac{E_C}{8E_J}}) < E_M < (8E_J E_C)/(E_C/2 + \sqrt{8E_J E_C})$, pairs of 2π phase slips bound forming 4π phase slips. However, the distance between the two 2π phase slips that form the 4π phase slip R (see Fig. 3) fluctuates.

(iii) *Bound 2π phase slips with fixed* **R**. For $E_M > (8E_J E_C)/(E_C/2 + \sqrt{8E_J E_C})$, the 4π tunneling is strong enough to bind pairs of 2π phase slips together and fix the distance between them R.

As will be further discussed in this section, the transition between neighboring regimes is not sharp. Both regimes will be valid in a region around these boundaries.

To further clarify the range of parameters in which each picture is valid, we compare the different effective models for the topological Josephson junction with numerical results. The spectrum of Eq. (10) is obtained numerically by truncating the Hilbert space in the number basis, where the Hamiltonian becomes

$$H = \sum_{n=-\infty}^{\infty} \left[E_C (n - n_g)^2 |n\rangle\langle n| - \frac{E_M}{4}(|n\rangle\langle n+1| + |n\rangle\langle n-1|) - \frac{E_J}{2}(|n\rangle\langle n+2| + |n\rangle\langle n-2|) \right]. \quad (33)$$
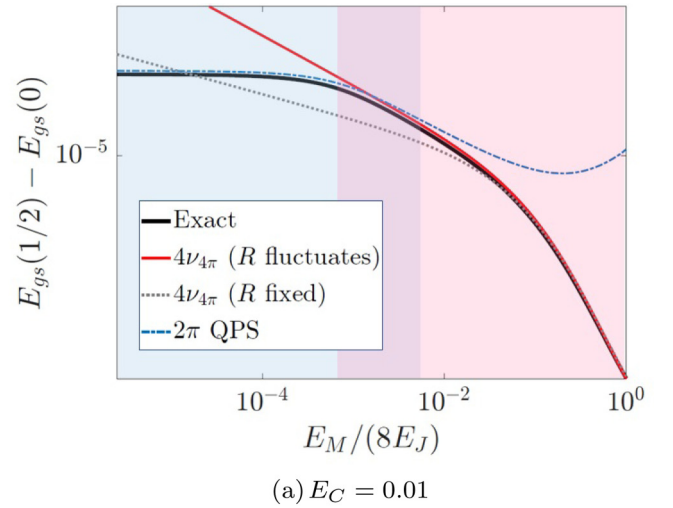
(a) $E_C = 0.01$
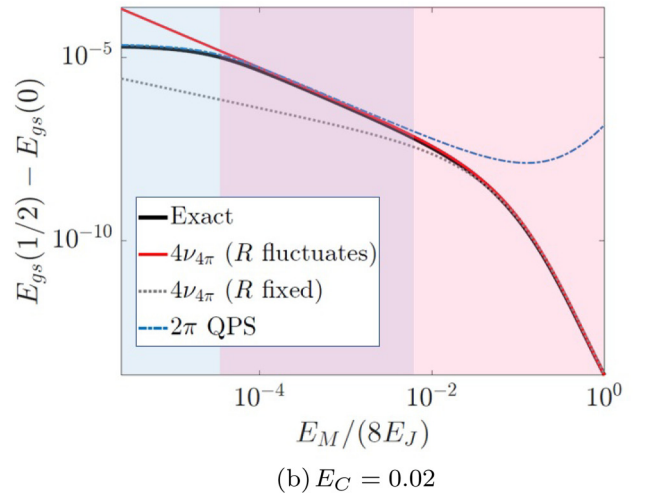
(b) $E_C = 0.02$

FIG. 5. The ground-state energy of the model as a function of the control parameter n_g depends on the phase slip probability. We therefore use the quantity $E_{gs}(1/2) - E_{gs}(0)$ to benchmark the effective models against numerical results (black solid line). If only 4π phase slips are present [Eq. (13)], $E_{gs}(1/2) - E_{gs}(0) = 4\nu_{4\pi}$. The different obtained expressions for $4\nu_{4\pi}$, Eqs. (16) (dotted gray) and Eqs. (17a)-(20) (solid red line), are shown. When 2π phase slips dominate [Eq. (24)], $E_{gs}(1/2) - E_{gs}(0) = (\sqrt{(\epsilon_o - \epsilon_e)^2 + (4\nu_{2\pi})^2} - |\epsilon_o - \epsilon_e|)/2$ with $\nu_{2\pi}$ given by Eq. (9) (blue dashed-dotted). The graphs are shown as a function of $E_M/(8E_J)$ with the sum $8E_J + E_M$ fixed at 1. The red shaded region corresponds well with the 4π phase slip scenario, while the blue shaded region denotes good agreement with the 2π phase slip scenario. The regions overlap where both approximations are close to the numerical data.

The numerical results shown in this paper are obtained by taking the sum in the above equation from $n = -N$ to $n = N$ with $N = 10^4$.

Comparisons between $E_{gs}(n_g)$ for the topological Josephson junction predicted by the effective models discussed previously and numerical results are shown in Fig. 5. The comparisons are done by plotting the difference $E_{gs}(1/2) - E_{gs}(0)$ as a function of $E_M/(8E_J)$ for different values of E_C. In Fig. 5 we have fixed $8E_J + E_M = 1$ such that $\hbar\omega$ is kept constant throughout each plot; this is done to show

the entire range of $E_M/(8E_J)$ in the same plot. As expected, when $E_M/(8E_J) \to 0$ the numerical results (solid black line) agree with the 2π QPS description (dotted-dashed blue line) provided by the tight-binding Hamiltonian, Eq. (22), while for larger values of $E_M/(8E_J)$ the 4π QPS description, i.e., that of Eq. (12), is closer to the numerical results. In addition, increasing E_C reduces the range of $E_M/(8E_J)$ in which the 4π QPS description is valid. This can be seen by comparing the two panels of Fig. 5.

Moreover, Fig. 5 shows the results of the 4π QPS description calculated in two ways. One scheme, commonly used in the literature, assumes that the distance between phase slips is fixed [Eq. (16), represented by gray dotted lines in Fig. 5]. This leads to a dispersion that agrees with the numerical data only for large ratios of $E_M/8E_J$. Since the 2π phase slip scenario is only appropriate at much smaller $E_M/8E_J$, an intermediate regime is unexplained by either scenario. To remedy this, we extend the 4π phase slip model to allow fluctuations of R [Eq. (17), red solid line in Fig. 5]. This extends the regime of validity of the model such that it overlaps with the 2π-phase slip scenario in the regime shaded in purple in both panels of Fig. 5.

We can use the numerical results to figure out the range of parameters in which each picture is more appropriate. This is shown in Fig. 1(a). As discussed previously, close to the boundary between the coupled 2π QPS and the 4π QPS regions, both descriptions give similar results.

V. CONNECTION WITH THE LARGE CHARGING ENERGY LIMIT

The above results indicate that the presence of local minima at odd multiples of 2π in the junction potential lead to a ground-state wave-function weight at odd multiples of 2π if E_C is large enough. A question that arises is whether the presence of local minima in the potential guarantees that there will be a large enough E_C such that the ground-state wave function is peaked at odd multiples of 2π. This can be answered by looking at the dominant charging energy limit.

For $E_M = E_J = 0$, the eigenstates of the junction have a well-defined particle number n, and their energies are given by $E_C(n - n_g)^2$. In the gauge where $\Psi(\theta + 4\pi) = \Psi(\theta)$, the phase-space wave functions of such states are given by $\Psi(\theta) = e^{-il\theta/2}$ with integer l. If $E_M, E_J \ll E_C$, the eigenstates of the junction can be found perturbatively from the well-defined number states. To first order in perturbation theory, the ground state of the junction for $n_g \in (-1/2, 1/2)$ is given by the unnormalized wave function

$$\Psi_{gs}(\theta) = 1 - \frac{E_M e^{-i\theta/2}}{4E_C(2n_g - 1)} + \frac{E_M e^{i\theta/2}}{4E_C(2n_g + 1)}$$
$$- \frac{E_J e^{-i\theta}}{8E_C(n_g - 1)} + \frac{E_J e^{i\theta}}{8E_C(n_g + 1)}. \quad (34)$$

The above wave function will be peaked at 2π if $|\Psi_{gs}(\theta)|$ has a local maximum at this point.

For simplicity, we focus on $n_g = 0$. In this case,

$$\Psi_{gs}(\theta) = 1 + \frac{E_M}{2E_C} \cos \frac{\theta}{2} + \frac{E_J}{4E_C} \cos \theta. \quad (35)$$

Since $E_M \ll E_C$ and $E_J \ll E_C$, then $\Psi_{gs}(\theta) = |\Psi_{gs}(\theta)|$. Looking at the derivatives of Ψ_{gs} at $\theta = 2\pi$, we find that 2π is a minimum of Ψ_{gs} when $E_M/(2E_J) > 1$ and a maximum when $E_M/(2E_J) < 1$. Therefore, the $n_g = 0$ ground-state wave function is peaked around odd multiples of 2π if $E_M/(2E_J) < 1$.

We see then that for $2E_J < E_M < 8E_J$ and $n_g = 0$, the ground-state wave function does not peak around odd multiples of 2π despite the junction having local potential minima there. Moreover, the wave-function weight around odd multiples of 2π is highest for integer values of n_g. This can be intuitively understood by noticing that the wave-function weight around odd multiples of 2π for half-integer n_g is strongly suppressed as a result of the degeneracy between the two nearby n states. Therefore, for any given n_g the ground-state wave function does not peak around odd multiples of 2π if $2E_J < E_M$. Then the presence of local minima in the potential does not guarantee that there will be a large enough value of E_C to cause a ground-state wave-function peak at odd multiples of 2π.

VI. DISCUSSION

In the previous sections, we found that for any ration of $E_M < 8E_J$ one might find both 4π and 2π phase slips, depending on the strength of the phase fluctuations given by E_C. Therefore, the scenario of 4π phase slips only is bound to fail for some value of E_C. We have estimated the value of E_C above which 2π phase slips dominate in the following way. First, we have evaluated the 4π phase slip probability $\nu_{4\pi}$ using a double sine-Gordon model. Well below the crossover line in Fig. 1(a), a double instanton classical solution with Gaussian quantum fluctuations yields Eq. (16). This equation fails at low E_M even before 2π phase slips take over due to a possible translational mode that was not taken into account. We improve the calculation in Eqs. (17), which does not have a closed-form solution but may be approximated in the subsequent equations. In the 2π phase slip dominated regime, we estimate $\nu_{2\pi}$ using a method for an asymmetric barrier and we arrive at Eqs. (25)–(29). Using both the 2π and 4π phase slip scenario, we generate plots for the energy difference $E_{gs}(n_g = 1/2) - E_{gs}(n_g = 0)$, which are compared with numerical solution for the problem in a truncated Hilbert space [using Eq. (33)]. The quality of the various approximations points to the crossover depicted in Fig. 1. A rough estimate of the crossover as a function of the problem's energy scales $x = E_M/8E_J$ and $y = E_C/8E_J$ can be found by comparing $\nu_{4\pi}$ and $\nu_{2\pi}$, which yields $x \propto \exp(-\alpha/\sqrt{y})$ with some slowly varying $\alpha(x)$.

It is interesting to discuss the implications of our results on the dissipative transition that is expected in this system [27,28,35]. This transition was previously studied in Ref. [35], where it was found that the presence of 4π periodic tunneling would reduce the Ohmic dissipation needed to restore superconductivity by a factor of 4. However, the results of Ref. [35] assumed that the topological junction could always be described by 4π QPS. In this work, we find that this is not necessarily the case. Consider a junction with fixed E_J and E_C. When $E_M = 0$ the junction is described by 2π QPS. Turning on E_M leads to coupling of these 2π QPS, which increases with E_M until they become confined into pairs. Following the

critical dissipation throughout this same path would lead to a continuous decrease in it until it reaches 1/4 of the original value at the point where the 2π QPS are fully suppressed. We also find that the critical dissipation needed to stabilize the superconductivity in our model of a topological Josephson junction is dependent on E_C.

An important caveat of using the dissipative phase transition as a mechanism for detecting Majorana modes is that the dissipation induced by quasiparticle tunneling also reduces the critical resistance of nontopological Josephson junctions by a factor of 4. Furthermore, the effects of dissipation induced by quasiparticle tunneling in nontopological Josephson junctions are dependent on the ratio between the Josephson coupling and the charging energy [28]. This is because both the 4π periodic tunneling induced by Majoranas and the quasiparticle tunneling are single-particle tunneling processes that break the same symmetry (the 2π periodicity of a nontopological Josephson junction), albeit the difference in coherence. A more careful analysis of dissipation in the topological Josephson junction is required to find whether there are signatures in the dissipative transition that would allow us to distinguish between the 4π periodic tunneling induced by Majoranas and the quasiparticle tunneling.

The difference in the effects of 4π periodic versus quasiparticle tunneling in the dissipative transition is unclear. However, the effects on the charge offset dispersion are clearly different. While both kinds of single-particle tunneling turn the system from 2π periodic to 4π periodic, the Majorana assisted tunneling opens up a gap [see Eq. (24)] while the quasiparticle tunneling does not [28]. This could be a potential probe to distinguish between the two kinds of single-particle tunneling.

Finally, another important issue to consider is the effect of quasiparticle poisoning in this system. Since instanton techniques tend to be useful to describe systems coupled to external environments [52], the formalism used in this work could be useful to study the effects of quasiparticle poisoning.

VII. CONCLUSIONS

We studied the effects of phase fluctuations induced by charging effects in a simple model of a topological Josephson junction. Our model considers both single-particle tunneling and pair tunneling, which are, respectively, 4π and 2π periodic with respect to the superconducting phase difference across the junction. We found that when the single-particle tunneling is a small component of the total tunneling current, there are two possible ways to describe the ground state of the junction: (i) in terms of 4π QPS or (ii) in terms of coupled 2π QPS. We found the tunneling amplitudes for both effective descriptions and compared them to numerical results to determine the range of parameter in which each description is appropriate. We note that in a real junction, one may not have control over the relative strength of E_M and E_J, and therefore observing 2π phase slips does not necessarily imply that the junction is not topological. However, if the junction is indeed topological and phase fluctuations can be reduced through capacitance (reducing E_C), 2π phase slips will be suppressed, revealing the topological nature of the junction.

In addition, we discussed the possible implications that our results have for the dissipative phase transition expected in this system. As was previously found by Ref. [35], when the ground state of the junction is described by 4π QPS, we expect the critical resistance needed to make the junction superconducting to be four times smaller than the critical resistance needed to make a nontopological junction superconducting. In the regime where tunneling processes between minima separated by 2π are still present in the system, we expect the critical transition to be somewhere between these two critical values. Given that increasing the charging energy of the junction may change the tunneling processes present in the system, our results also point toward a charging energy dependence of the critical resistance for the dissipative transition.

Several questions regarding the dissipative transition, particularly in relation to quasiparticle tunneling, remain unanswered. In the future, we will use the formalism developed in this work to obtain a quantitative description of this transition. It would also be interesting to pinpoint the relation between the results presented in this work and the dominant charging energy limit.

APPENDIX A: PATH INTEGRAL CALCULATIONS

1. 4π phase slip amplitude

The calculation of the tunneling amplitude between the different potential minima can be performed using standard semiclassical methods. We include the calculation here in detail for completeness, largely following Ref. [44].

We begin by calculating the amplitude to propagate from 0 to 4π in an imaginary-time interval $2L$. This is given by the following path integral:

$$(0, -L|4\pi, L) = \int [\mathcal{D}\theta] e^{-\frac{1}{\hbar} \int_{-L}^{L} \mathcal{L}[\theta(\tau)]d\tau}, \quad (A1)$$

where $\mathcal{L}(\tau)$ is the double sine-Gordon (DSG) Lagrangian given by Eq. (14), which can be rewritten as

$$\mathcal{L}(\theta) = M\left(\frac{(\partial_\tau\theta)^2}{2} + V(\theta)\right) \quad (A2)$$

with

$$V(\theta) = \omega^2\left[\tanh^2 R(1 - \cos\theta) + 4\,\text{sech}^2 R\left(1 - \cos\frac{\theta}{2}\right)\right] \quad (A3)$$

and

$$M = \hbar^2/(8E_C),$$
$$\omega = \sqrt{E_C(8E_J + E_M)}/\hbar, \quad (A4)$$
$$\cosh(R) = \sqrt{(8E_J + E_M)/E_M}.$$

We expect the leading contribution to the path integral to be from paths of the form

$$\theta(\tau) = \theta^{\mathrm{cl}}(\tau) + \chi(\tau), \tag{A5}$$

where $\theta^{\mathrm{cl}}(\tau)$ is the classical path, which minimizes the action and interpolates between $\theta = 0$ at $\tau = -L$ and $\theta = 4\pi$ at $\tau = L$. $\chi(\pm L) = 0$ is the deviation from the classical path, and $\theta^{\mathrm{cl}}(\tau)$ fulfills the following equation:

$$\frac{dV}{d\theta}[\theta^{\mathrm{cl}}(\tau)] = \frac{d^2\theta^{\mathrm{cl}}}{d\tau^2}. \tag{A6}$$

In the limit $L \to \infty$, $\theta^{\mathrm{cl}}(\tau)$ is given by

$$\theta^{\mathrm{cl}} = 4\arctan\left[e^{\omega(\tau-\tau_0)+R}\right] + 4\arctan\left[e^{\omega(\tau-\tau_0)-R}\right]. \tag{A7}$$

Up to second order in $\chi(\tau)$, the Lagrangian for paths of the form Eq. (A5) is

$$\mathcal{L}(\theta) = \mathcal{L}(\theta^{\mathrm{cl}}) + \frac{M}{2}(\partial_\tau\chi)^2 + \frac{M}{2}\frac{d^2V}{d\theta^2}(\theta^{\mathrm{cl}})\chi^2 + M\partial_\tau(\chi\partial_\tau\theta^{\mathrm{cl}}). \tag{A8}$$

This allows us to split the path integral in Eq. (A1) into two parts:

$$(0, -L|4\pi, L) \approx F\exp\left(-\frac{S^{\mathrm{cl}}}{\hbar}\right) \tag{A9}$$

with S^{cl} the action of the instanton,

$$S^{\mathrm{cl}} = \int_{-L}^{L} d\tau\, \mathcal{L}(\theta^{\mathrm{cl}}), \tag{A10}$$

and F contains the sum over Gaussian fluctuations around such an instanton. F can be written as

$$F = \int [\mathcal{D}\chi] \exp\left(-\frac{M}{2\hbar}\int_{-L}^{L} d\tau\, \chi D\chi\right), \tag{A11}$$

with D is the following differential operator:

$$D = -\frac{d^2}{d\tau^2} + \frac{d^2V}{d\theta^2}[\theta^{\mathrm{cl}}(\tau)]. \tag{A12}$$

The path integral in Eq. (A11) can be solved expanding χ in terms of the eigenfunctions of the operator D, i.e., taking

$$\chi(\tau) = \sum_n \chi_n y_n(\tau) \tag{A13}$$

with

$$D y_n(\tau) = \lambda_n y_n. \tag{A14}$$

This leads to

$$F = \mathcal{N}\prod_n \int_{-\infty}^{\infty} \frac{d\chi_n}{\sqrt{2\pi\hbar/M}} e^{-\frac{M\lambda_n\chi_n^2}{2\hbar}} \tag{A15}$$

with $\mathcal{N}$ a normalization constant. However, the above expression in not well-defined since the operator D contains a zero mode, λ_0, which leads to a divergence in F. The time τ_0 at which the kink solution is centered is arbitrary, which leads to $D\partial_\tau\theta^{\mathrm{cl}} = 0$, i.e., the zero mode is a consequence of the time-translational invariance of the system. To deal with this divergence, we use the Fadeev-Popov method to transform the χ_0 integration to a τ_0 integration.

The Fadeev-Popov method consists of inserting

$$1 = \int d\tau_0 \left|\frac{\partial\chi_0}{\partial\tau_0}(\chi_0 = 0)\right| \delta(\chi_0) \tag{A16}$$

into the expression for F given by Eq. (A15):

$$\begin{aligned}
F &= \mathcal{N}\prod_{n=1}^{\infty} \int_{-\infty}^{\infty} \frac{d\chi_n}{\sqrt{2\pi\hbar/M}} e^{-\frac{M\lambda_n\chi_n^2}{2\hbar}} \int d\tau_0 \left|\frac{\partial\chi_0}{\partial\tau_0}(\chi_0 = 0)\right| \\
&\quad \times \int \frac{d\chi_0}{\sqrt{2\pi\hbar/M}}\delta(\chi_0) \\
&= \mathcal{N}\prod_{n=1}^{\infty} \int_{-\infty}^{\infty} \frac{d\chi_n}{\sqrt{2\pi\hbar/M}} e^{-\frac{M\lambda_n\chi_n^2}{2\hbar}} \int \frac{d\tau_0}{\sqrt{2\pi\hbar/M}} \left|\frac{\partial\chi_0}{\partial\tau_0}(\chi_0 = 0)\right|.
\end{aligned} \tag{A17}$$

The Jacobian $\left|\frac{\partial\chi_0}{\partial\tau_0}(\chi_0 = 0)\right|$ can be found rewriting the path θ so that fluctuations in the direction of the zero mode are traded for an explicit τ_0 dependence:

$$\theta(\tau) = \theta^{\mathrm{cl}}(\tau - \tau_0) + \sum_{n=1}^{\infty} \chi_n y_n(\tau - \tau_0). \tag{A18}$$

Comparing the above expression for the path with that of Eq. (A5) leads to

$$\chi_0 = f(\tau_0) + \sum_{m=1}^{\infty} \xi_m r_n(\tau_0) \tag{A19}$$

with

$$\begin{aligned}
f(\tau_0) &= \int d\tau[\theta^{\mathrm{cl}}(\tau - \tau_0) - \theta^{\mathrm{cl}}(\tau)]y_0(\tau), \\
r_m(\tau_0) &= \int d\tau\, y_m(\tau - \tau_0)y_0(\tau). \tag{A20}
\end{aligned}$$

Furthermore, we note that the constraint $\chi_0 = 0$ corresponds to $\tau_0 = 0$, so we obtain

$$\left|\frac{\partial\chi_0}{\partial\tau_0}(\chi_0 = 0)\right| = \left|f'(0) + \sum_{m=1}^{\infty} \xi_m r_m'(0)\right|. \tag{A21}$$

We know $\partial_\tau\theta^{\mathrm{cl}} \propto y_0(\tau)$ since $D\partial_\tau\theta^{\mathrm{cl}} = 0$. The proportionality constant can be found using the following expression:

$$\int_{-\infty}^{\infty} d\tau(\partial_\tau\theta^{\mathrm{cl}})^2 = \frac{S^{\mathrm{cl}}}{M}, \tag{A22}$$

which stems from the fact that $\theta^{\mathrm{cl}}(\tau)$ minimizes the action [Eq. (A6)]. We use this to find $f'(0)$:

$$f'(0) = -\int d\tau\, \partial_\tau\theta^{\mathrm{cl}}(\tau)y_0(\tau) = -\sqrt{\frac{S^{\mathrm{cl}}}{M}}. \tag{A23}$$

The appropriate boundaries of integration for τ_0 are $-L$ and L since τ takes values in the interval $(-L, L)$. We then obtain

$$\begin{aligned}
F &= \mathcal{N}\prod_{n=1}^{\infty} \int_{-\infty}^{\infty} \frac{d\chi_n}{\sqrt{2\pi\hbar/M}} e^{-\frac{M\lambda_n\chi_n^2}{2\hbar}} \\
&\quad \times \int_{-L}^{L} \frac{d\tau_0}{\sqrt{2\pi\hbar/M}}\left(\sqrt{\frac{S^{\mathrm{cl}}}{M}} - \sum_{m=1}^{\infty} \xi_m r_m'(0)\right) \\
&= \mathcal{N}2L\sqrt{\frac{S^{\mathrm{cl}}}{2\pi\hbar}}\frac{1}{\sqrt{\prod'_n \lambda_n}}, \tag{A24}
\end{aligned}$$

where $\prod_n'$ indicates the product over the eigenvalues taking out the zero eigenvalue.

The normalization constant can be conveniently expressed in terms of the sum over harmonic fluctuations around 0 or 4π. If we define

$$F_0 = \int [\mathcal{D}\chi] \exp\left(-\frac{M}{2\hbar} \int_{-L}^{L} d\tau \, \chi D_0 \chi\right) \quad (A25)$$

with

$$D_0 = -\frac{d^2}{d\tau^2} + \omega^2, \quad (A26)$$

the normalization constant $\mathcal{N}$ can be written as

$$\mathcal{N} = F_0 \sqrt{\prod_n \lambda_n^0}, \quad (A27)$$

where λ_n^0 are the eigenvalues of the differential operator D_0. F_0, the fluctuation contribution to the imaginary-time harmonic-oscillator propagator, is readily available in the literature (see, e.g., Ref. [44]). For $L \to \infty$, its leading contribution is

$$F_0 = \sqrt{\frac{M\omega}{\pi\hbar}} e^{-\omega L}. \quad (A28)$$

Our expression for F currently includes a ratio between the products of eigenvalues of the operators D_0 and D:

$$F = 2LF_0 \sqrt{\frac{S^{\mathrm{cl}}}{2\pi\hbar}} \sqrt{\frac{\prod_n \lambda_n^0}{\prod_n' \lambda_n}}, \quad (A29)$$

which can be evaluated using the Gelfand-Yaglom formula. Following Ref. [44], we have

$$\frac{\prod_n \lambda_n^0}{\prod_n' \lambda_n} = \frac{2M\omega\eta^2}{S^{\mathrm{cl}}}, \quad (A30)$$

where η is defined by the asymptotic behavior of the classical solution:

$$\partial_\tau \theta^{\mathrm{cl}} \to \eta e^{-\omega|\tau|} \quad \text{for} \quad \tau \to \pm\infty. \quad (A31)$$

To the leading order, the amplitude to propagate from 0 to 4π in an imaginary-time interval $2L$ is then

$$(0, -L|4\pi, L) \approx 2LF_0 \eta \sqrt{\frac{M\omega}{\pi\hbar}} e^{-\frac{S^{\mathrm{cl}}}{\hbar}}. \quad (A32)$$

However, the leading-order contribution is not enough to obtain the level splitting. It is possible to obtain a more precise expression for the amplitude using the dilute instanton gas approximation.

Under the dilute instanton gas approximation, we sum over paths consisting of combinations of kinks and antikinks and quadratic fluctuations around them, i.e.,

$$\theta(\tau) = \sum_{n=0}^{2N} v_n \theta^{\mathrm{cl}}(\tau - \tau_n) + \chi(\tau), \quad (A33)$$

where $v_n = \pm 1$ ($+$ for kinks and $-$ for antikinks) and $\sum_n v_n = 1$. The approximation consists of considering that the centers of the kinks and antikinks, i.e., τ_n, are sufficiently spread out to make kink-kink interactions negligible. The obtained result is

$$(0, -L|4\pi, L) = \sum_n \frac{F_0 \left(2L\eta \sqrt{\frac{M\omega}{\pi\hbar}} e^{-\frac{S^{\mathrm{cl}}}{\hbar}}\right)^{2n+1}}{(2n+1)!}$$

$$= F_0 \sinh\left(2L\eta \sqrt{\frac{M\omega}{\pi\hbar}} e^{-\frac{S^{\mathrm{cl}}}{\hbar}}\right). \quad (A34)$$

The spectral representation of the amplitude in Eq. (A1) is

$$(0, -L|4\pi, L) = \sum_n \psi_n(0)\psi_n(4\pi) e^{-2LE_n/\hbar}. \quad (A35)$$

Considering two ground-state levels of harmonic oscillators with frequency ω and mass M, one centered around 0 and the other around 4π, which can tunnel to each other with amplitude v, we have

$$\psi_1(\theta) = \frac{1}{\sqrt{2}}[\psi_0(\theta) + \psi_{4\pi}(\theta), \quad E_1 = \frac{\hbar\omega}{2} - v,$$

$$\psi_2(\theta) = \frac{1}{\sqrt{2}}[\psi_0(\theta) - \psi_{4\pi}(\theta)], \quad E_2 = \frac{\hbar\omega}{2} + v. \quad (A36)$$

In the above expressions, $\psi_0(\theta)$ and $\psi_{4\pi}(\theta)$ are the ground-state wave functions of harmonic oscillators centered around 0 and 4π, respectively, e.g.,

$$\psi_0(\theta) = \left(\frac{M\omega}{\pi\hbar}\right)^{1/4} e^{-\frac{M\omega\theta^2}{2\hbar}}. \quad (A37)$$

The amplitude, Eq. (A1), for such a system would then be

$$(0, -L|4\pi, L) = \sqrt{\frac{M\omega}{\pi\hbar}} e^{-L\omega} \sinh(2Lv/\hbar). \quad (A38)$$

Comparing Eqs. (A34) and (A38) allows us to conclude

$$v = \hbar\eta \sqrt{\frac{M\omega}{\pi\hbar}} \exp\left(-\frac{S^{\mathrm{cl}}}{\hbar}\right). \quad (A39)$$

For the kink in Eq. (A7) we have

$$S^{\mathrm{cl}} = 16M\omega(1 + 2R\operatorname{csch}2R), \quad \eta = 8\omega\cosh R. \quad (A40)$$

Substituting the values of M, ω, and R from Eq. (A4), we obtain

$$v_{4\pi} = \sqrt{\frac{8(\hbar\omega)^5}{\pi E_M E_C^2}} \exp\left[-\frac{\hbar\omega}{E_C} \times f\left(\frac{E_M}{8E_J}\right)\right] \quad (A41)$$

with

$$f(x) = 2 + \frac{2x}{\sqrt{1+x}} \coth^{-1}(\sqrt{1+x}). \quad (A42)$$

2. Emergent translational mode correction for the 4π phase slip amplitude

Here, we follow the procedure outlined in Ref. [51] to introduce corrections to the previously found expression for $v_{4\pi}$. This section then follows the work done in Ref. [51] closely. We include the calculation here for clarity, as the work in Ref. [51] was done in the context of classical statistical mechanics. We also note that Ref. [51] claims, incorrectly,

that this procedure leads to a nondivergent expression. Here, we find otherwise.

When $E_M \to 0$, the expression for ν found in (A 1) diverges. This occurs because one of the eigenmodes of the operator D, which we will call λ_1, approaches 0 when $E_M \to 0$. Physically, the two 2π kinks decouple, turning the distance between the two 2π kinks $2R$ into another translation mode. We must then have

$$y_1(\tau) \to \partial_R(\theta^{\mathrm{cl}}) \quad \text{when} \quad E_M \to 0. \quad (A43)$$

This means that we can deal with the effects of the emergent translational mode by writing the path as

$$\theta(\tau) = \theta^{\mathrm{cl}}(\tau) + \sum_{n=0}^{\infty} \chi_n y_n(\tau)$$

$$= \sigma(\tau - \tau_0, r) + \sum_{n=2}^{\infty} \chi_n y_n(\tau - \tau_0) \quad (A44)$$

with

$$\sigma(\tau, r) = 4 \arctan[e^{\omega\tau + r}] + 4 \arctan[e^{\omega\tau - r}]. \quad (A45)$$

For $R = r$ we recover the classical solution, i.e., $\sigma(\tau, R) = \theta^{\mathrm{cl}}(\tau)$. We should note that Eq. (A44), and therefore the rest this Appendix, relies on $y_1 \approx \partial_R(\theta^{\mathrm{cl}})$. This is a valid assumption when $R > 1.25$ [50,51].

Up to second order in $\chi = \sum_{n=2}^{\infty} \chi_n y_n(\tau - \tau_0) = 0$, the Lagrangian for the above path is given by

$$\frac{\mathcal{L}(\sigma, \chi)}{M} = \frac{(\partial_\tau \sigma + \partial_\tau \chi)^2}{2} + V_0(\sigma) + \chi V_1(\sigma) + \chi^2 V_2(\sigma), \quad (A46)$$

where $V_0(\sigma) = V(\sigma)$ is the potential of σ given by Eq. (A3), and

$$V_1(\sigma) = \frac{\omega^2}{\cosh^2(R)} \left(\sinh^2(R) \sin \sigma + 2 \sin \frac{\sigma}{2} \right),$$

$$V_2(\sigma) = \frac{\omega^2}{\cosh^2(R)} \left(\frac{1}{2} \sinh^2(R) \cos \sigma + \frac{1}{2} \cos \frac{\sigma}{2} \right). \quad (A47)$$

The action of this path can be written as

$$S(\sigma, \chi) = S_0(r) + S_1(\sigma, \chi) \quad (A48)$$

with $S_0(r)$ and $S_1(\sigma, \chi)$ given by

$$S_0(r) = M \int d\tau \left(\frac{1}{2} (\partial_\tau \sigma)^2 + V_0(\sigma) \right)$$

$$= 8M\omega \left(1 + \frac{\tanh^2 R}{\tanh^2 r} + \frac{2r}{\sinh 2r} + \frac{2r \coth r}{\cosh^2 R} - \frac{r \tanh^2 R \coth r}{\sinh^2 r} \right),$$

$$S_1(\sigma, \chi) = M \int d\tau [-\partial_\tau \sigma + V_1(\sigma)] \chi$$

$$+ M \int d\tau \left(\frac{1}{2} (\partial_\tau \chi)^2 + V_2(\sigma) \chi^2 \right). \quad (A49)$$

Using the Fadeev-Popov method to transform from the coordinates χ_0 and χ_1 to τ_0 and r leads to

$$(0, -L|4\pi, L) = \mathcal{N} \iint \frac{d\tau_0 dr}{2\pi \hbar/M} \left| \frac{\partial \chi_0 \partial \chi_1}{\partial \tau_0 \partial r} \right| \Big|_{\chi_0, \chi_1 = 0}$$

$$\times \prod_{n=2}^{\infty} \int \frac{d\chi_n}{\sqrt{2\pi \hbar/M}} e^{-S_0(r)/\hbar - S_1(\sigma, \chi)/\hbar}. \quad (A50)$$

Following Ref. [51], we make the approximations

$$\left| \frac{\partial \chi_0 \partial \chi_1}{\partial \tau_0 \partial r} \right| \Big|_{\chi_0, \chi_1 = 0} \approx \sqrt{\int d\tau (\partial_\tau \sigma)^2 \times \int d\tau (\partial_r \sigma)^2}$$

$$\times \int \prod_{n=2}^{\infty} \frac{d\chi_n}{\sqrt{2\pi \hbar/M}} e^{-S_1(\sigma, \chi)/\hbar}$$

$$\approx \frac{1}{\sqrt{\prod_n'' \lambda_n}}, \quad (A51)$$

where the λ_n's are the eigenmodes of the operator $\mathcal{D}$ from Eq. (A12), and the product $\prod_n''$ skips the 0 eigenmode and λ_1.

Under these approximations, we can write

$$(0, -L|4\pi, L) = F'K2L \quad (A52)$$

with

$$F' = \frac{\mathcal{N}}{\sqrt{\prod_n'' \lambda_n}} = F_0 \sqrt{\frac{\prod_n \lambda_n^0}{\prod_n'' \lambda_n}} = F_0 \eta \sqrt{\frac{2M\omega}{S^{\mathrm{cl}}}} \sqrt{\lambda_1} \quad (A53)$$

and

$$K = \int_0^{L\omega} dr \frac{M \sqrt{\int d\tau (\partial_\tau \sigma)^2 \times \int d\tau (\partial_r \sigma)^2}}{2\pi \hbar}$$

$$\times e^{-S_0(r)/\hbar} \int_{-L + \frac{r}{\omega}}^{L - \frac{r}{\omega}} \frac{d\tau_0}{2L}. \quad (A54)$$

Using the following result from Ref. [50]:

$$\sqrt{\int d\tau (\partial_\tau \sigma)^2 \times \int d\tau (\partial_r \sigma)^2} = 16\sqrt{1 - 4r^2 \mathrm{csch}^2 2r} \quad (A55)$$

and performing the τ_0 integration gives

$$K = \int_0^{L\omega} dr \frac{16M(\omega L - r)\sqrt{1 - 4r^2 \mathrm{csch}^2 2r}}{2\pi \hbar \omega L} e^{\frac{-S_0(r)}{\hbar}}. \quad (A56)$$

It is possible to calculate λ_1 by noting that calculating K using a quadratic approximation on $\rho = r - R$ gives

$$K_0 = \sqrt{\frac{S^{\mathrm{cl}}}{2\pi \hbar}} \frac{1}{\sqrt{\lambda_1}} e^{-\frac{S^{\mathrm{cl}}}{\hbar}}. \quad (A57)$$

Expanding $S_0(r)$ up to second order in ρ leads to

$$S_0(\rho) = S^{\mathrm{cl}} + 2M\omega\rho^2 \mathrm{csch}^3 R \, \mathrm{sech}^3 R(4 \sinh 2R - 4R + \sinh 4R - 8R \cosh 2R). \quad (A58)$$

We then find

$$K_0 = \int_{-\infty}^{\infty} d\rho \, \frac{M 16\sqrt{1 - 4R^2 \text{csch}^2 2R}}{2\pi\hbar} e^{-\frac{S_0(\rho)}{\hbar}}$$

$$= \sqrt{\frac{M}{\hbar\omega\pi}} g(R) e^{-\frac{S^{\text{cl}}}{\hbar}} \tag{A59}$$

with

$$g(R) = \frac{\sinh 2R \sqrt{2 - 8R^2 \text{csch}^2 2R}}{\sqrt{\cosh 2R - R\tanh R - 3R\coth R + 2}}. \tag{A60}$$

Note that the factor $(1 - \frac{r}{L})$ from Eq. (A56) goes to 1 in Eq. (A59) as we are taking the $L \to \infty$ limit. The vanishing eigenvalue λ_1 is then

$$\sqrt{\lambda_1} = \sqrt{\frac{S^{\text{cl}}}{2\pi\hbar}} \frac{e^{-\frac{S^{\text{cl}}}{\hbar}}}{K_0} = \sqrt{\frac{S^{\text{cl}}\omega}{2M}} \frac{1}{g(R)}, \tag{A61}$$

which leads to

$$(0, -L|4\pi, L) = 2LF_0 \frac{\eta\omega}{g(R)} K. \tag{A62}$$

Using the dilute instanton gas approximation (see the previous section), this result leads to the tunneling amplitude

$$\nu_{4\pi} = \hbar \frac{\eta\omega}{g(R)} K = \frac{8\hbar\omega^2 \cosh R}{g(R)} K. \tag{A63}$$

Taking L to infinity results in

$$K = \frac{8M}{\pi\hbar} \mathcal{I}\left(R, \frac{\hbar\omega}{E_C}\right) = \frac{\hbar}{\pi E_C} \mathcal{I}\left(R, \frac{\hbar\omega}{E_C}\right), \tag{A64}$$

with $\mathcal{I}(R, \alpha)$ defined by Eq. (17c). Our final expression for ν is

$$\nu = \frac{8(\hbar\omega)^2 \cosh R}{g(R)\pi E_C} \mathcal{I}\left(R, \frac{\hbar\omega}{E_C}\right), \tag{A65}$$

which corresponds to Eq. (17) in the main text since $F(R) = 2\cosh R/g(R)$.

APPENDIX B: APPROXIMATE EXPRESSIONS FOR $\mathcal{I}(R, \alpha)$

1. Validity of the harmonic approximation

Taking $r = R + y/\sqrt{\alpha S_R''(R)}$, we can write the saddle-point expansion of $\mathcal{I}(R, \alpha)$ as

$$\mathcal{I}(R, \alpha) \approx \int_{-\infty}^{\infty} \frac{dy \sqrt{1 - 4R^2 \text{csch}^2 2R} e^{-\alpha S_R(R)}}{\sqrt{\alpha S_R''(R)}}$$

$$\times e^{-y^2/2}\left(1 + \sum_{n=1}^{\infty} \frac{p_n(y, R)}{[\alpha S_R''(R)]^{n/2}}\right)$$

$$= e^{-\alpha S_R(R)} \sqrt{\frac{2\pi(1 - 4R^2 \text{csch}^2 2R)}{\alpha S_R''(R)}}$$

$$\times \left(1 + \sum_{n=1}^{\infty} \frac{C_n(R)}{[\alpha S_R''(R)]^n}\right). \tag{B1}$$

In the above equation, the $p_n(y, R)$ are odd/even polynomials in y when n is even/odd, and the $C_n(R)$ are functions of R,

which can be expressed in terms of derivatives of $S_R(r)$ and $\sqrt{1 - 4r^2 \text{csch}^2 2r}$ evaluated at $r = R$.

The expression for $\mathcal{I}(R, \alpha)$ in Eq. (20) corresponds to the first term in the above saddle-point expansion; therefore, it is a valid approximation if $1/[\alpha S_R''(R)] \ll 1$. The function $1/S_R''(R)$ diverges for $R \to 0$ and for $R \to \infty$ making the approximation for both small and large R. However, since Eq. (17) was obtained to address the large-R divergence, we only need to find the upper R limit for the validity of Eq. (20). Since

$$\frac{1}{\alpha S_R''(R)} = \frac{e^{2R}}{16\alpha} + O(R), \tag{B2}$$

Eq. (20) is valid when $e^{2R} \ll 16\alpha$. This condition makes the tunneling expression of Eq. (16) valid for $E_M/(8E_J) \gg E_C/(4\hbar\omega)$.

2. Large-R limit

To find an approximate expression for $\mathcal{I}(R, \alpha)$ in the large-R limit, we note that $S_R(r)$ grows linearly with r for large r. Furthermore, the slope of the large-r linear behavior increases as R increases. This means that, when R is large, the largest contribution to $\mathcal{I}(R, \alpha)$ will come from the large-r linear behavior. We start by writing the following large r expansions:

$$S_R(r) = 1 + \tanh^2 R + 2r\,\text{sech}^2 R + 4e^{-2r}(2r\,\text{sech}^2 R$$

$$+ \tanh^2 R) + O(e^{-4r})\sqrt{1 - 4r^2 \text{csch}^2 2r}$$

$$= 1 + O(e^{-4r}). \tag{B3}$$

This means we can expand $\mathcal{I}(R, \alpha)$ as

$$\mathcal{I}(R, \alpha) = \int_0^{\infty} dr \, e^{-\alpha(1 + \tanh^2 R + 2r\,\text{sech}^2 R)}(1 - \alpha 4e^{-2r}$$

$$\times (2r\,\text{sech}^2 R + \tanh^2 R) + O(e^{-4r}))$$

$$= \mathcal{I}_0(R, \alpha) + \mathcal{I}_1(R, \alpha) + \cdots, \tag{B4}$$

where

$$\mathcal{I}_0(R, \alpha) = \frac{\cosh^2 R e^{-\alpha(\tanh^2 R + 1)}}{2\alpha} \tag{B5}$$

corresponds to the approximation to $\mathcal{I}(R, \alpha)$ cited in Eq. (18) and $\mathcal{I}_1(R, \alpha)$ is a leading-order correction that we calculate to determine the range of validity of Eq. (18).

Performing the r interaction gives

$$\mathcal{I}_1(R, \alpha) = \frac{-2\alpha(\alpha\tanh^2 R\,\text{sech}^2 R + 1)e^{-\alpha\tanh^2 R - \alpha}}{(\alpha\,\text{sech}^2 R + 1)^2}, \tag{B6}$$

and we obtain

$$\frac{\mathcal{I}_1(R, \alpha)}{\mathcal{I}_0(R, \alpha)} \sim 16\alpha^2 e^{-2R} \sim 4\alpha^2 \frac{E_M}{8E_J}. \tag{B7}$$

The approximation is valid when $16\alpha^2 e^{-2R} \ll 1$. For R given by Eq. (15b) and $\alpha = \hbar\omega/E_C$, this is equivalent to $E_M/(8E_J) \ll 0.25 E_C^2/(\hbar\omega)^2$.

For $\mathcal{I}(R, \alpha) \approx \mathcal{I}_0(R, \alpha)$, we obtain

$$\nu_{4\pi} = \frac{f_2\left(\frac{E_M}{8E_J}\right)(\hbar\omega)^3}{\pi E_C E_M} \exp\left[-\frac{\hbar\omega}{E_C} \times f_1\left(\frac{E_M}{8E_J}\right)\right] \tag{B8}$$

with

$$f_1(x) = \frac{2+x}{1+x}, \quad f_2(x) = \left[\frac{6(x+1)}{\frac{x}{\sqrt{x+1}} \log\left(\frac{\sqrt{x+1}+1}{\sqrt{x}}\right) + 1} + \frac{2}{\frac{x}{\sqrt{x+1}} \log\left(\frac{\sqrt{x+1}+1}{\sqrt{x}}\right) - 1} \right]^{1/2}. \quad \text{(B9)}$$

APPENDIX C: DECOUPLING OF 4π PHASE SLIPS

As has been previously noted, the expression for $\nu_{4\pi}$ in Eq. (19) diverges when $E_M \to 0$. In this appendix, we will show that it is possible to recover the decoupling of the 4π phase slips into two 2π phase slips from Eq. (A63). This is achieved by changing the order in which the limits $E_M \to 0$ and $L \to 0$ are taken.

Expanding F' and K around $x = E_M/(8E_J) = 0$ leads to

$$F' = F_0 \omega^2 \left\{ 4 + x \left[3 - 2 \log\left(\frac{x}{4}\right) \right] + O(x^2) \right\}$$

$$K = \frac{4LM\omega e^{-\frac{16M\omega}{\hbar}}}{\pi\hbar} - \frac{16x\left(2LM^2\omega^2(2L\omega - 3)e^{-\frac{16M\omega}{\hbar}}\right)}{3(\pi\hbar^2)}$$

$$+ O(x^2). \quad \text{(C1)}$$

Then, when $E_M \to 0$,

$$(0, -L|4\pi, L) \to F_0 \frac{8(2L)^2 M\omega^3 e^{-\frac{16M\omega}{\hbar}}}{\pi\hbar}. \quad \text{(C2)}$$

The tunneling amplitude between 0 and 2π in a nontopological Josephson junction can be written as

$$\nu_{2\pi} = 4\omega \sqrt{\frac{\hbar M\omega}{\pi}} e^{-\frac{8M\omega}{\hbar}}. \quad \text{(C3)}$$

This leads to

$$(0, -L|4\pi, L) \to F_0 \frac{(2L)^2}{2} \left(\frac{\nu_{2\pi}}{\hbar}\right)^2, \quad \text{(C4)}$$

which is the expected result for propagating between 0 to 4π through two uncoupled 2π phase slips. The $\frac{1}{2}$ factor arises from time ordering the phase slips, i.e.,

$$\int_{-L}^{L} d\tau_1 \int_{\tau_1}^{L} d\tau_2 = \frac{(2L)^2}{2}. \quad \text{(C5)}$$

[1] T. Senthil, Annu. Rev. Condens. Matter Phys. **6**, 299 (2015).

[2] F. D. M. Haldane, Rev. Mod. Phys. **89**, 040502 (2017).

[3] R. M. Lutchyn, J. D. Sau, and S. Das Sarma, Phys. Rev. Lett. **105**, 077001 (2010).

[4] Y. Oreg, G. Refael, and F. von Oppen, Phys. Rev. Lett. **105**, 177002 (2010).

[5] R. Aguado, Riv. Nuovo Cimento **40**, 523 (2017).

[6] S. D. Sarma, M. Freedman, and C. Nayak, Npj Quantum Inf. **1**, 15001 (2015), review article.

[7] A. Y. Kitaev, Phys. Usp. **44**, 131 (2001).

[8] S. M. Albrecht, A. P. Higginbotham, M. Madsen, F. Kuemmeth, T. S. Jespersen, J. Nygård, P. Krogstrup, and C. M. Marcus, Nature (London) **531**, 206 (2016).

[9] Ö. Gül, H. Zhang, J. D. S. Bommer, M. W. A. de Moor, D. Car, S. R. Plissard, E. P. A. M. Bakkers, A. Geresdi, K. Watanabe, T. Taniguchi, and L. P. Kouwenhoven, Nat. Nanotechnol. **13**, 192 (2018).

[10] M. T. Deng, S. Vaitiekenas, E. B. Hansen, J. Danon, M. Leijnse, K. Flensberg, J. Nygård, P. Krogstrup, and C. M. Marcus, Science **354**, 1557 (2016).

[11] A. D. K. Finck, D. J. Van Harlingen, P. K. Mohseni, K. Jung, and X. Li, Phys. Rev. Lett. **110**, 126406 (2013).

[12] A. Das, Y. Ronen, Y. Most, Y. Oreg, M. Heiblum, and H. Shtrikman, Nat. Phys. **8**, 887 (2012).

[13] H. O. H. Churchill, V. Fatemi, K. Grove-Rasmussen, M. T. Deng, P. Caroff, H. Q. Xu, and C. M. Marcus, Phys. Rev. B **87**, 241401 (2013).

[14] M. T. Deng, C. L. Yu, G. Y. Huang, M. Larsson, P. Caroff, and H. Q. Xu, Nano Lett. **12**, 6414 (2012).

[15] V. Mourik, K. Zuo, S. M. Frolov, S. R. Plissard, E. P. A. M. Bakkers, and L. P. Kouwenhoven, Science **336**, 1003 (2012).

[16] L. P. Rokhinson, X. Liu, and J. K. Furdyna, Nat. Phys. **8**, 795 (2012).

[17] T. Hyart, B. van Heck, I. C. Fulga, M. Burrello, A. R. Akhmerov, and C. W. J. Beenakker, Phys. Rev. B **88**, 035121 (2013).

[18] K. Flensberg, Phys. Rev. Lett. **106**, 090503 (2011).

[19] P. Bonderson and R. M. Lutchyn, Phys. Rev. Lett. **106**, 130505 (2011).

[20] B. van Heck, A. R. Akhmerov, F. Hassler, M. Burrello, and C. W. J. Beenakker, New J. Phys. **14**, 035019 (2012).

[21] D. Aasen, M. Hell, R. V. Mishmash, A. Higginbotham, J. Danon, M. Leijnse, T. S. Jespersen, J. A. Folk, C. M. Marcus, K. Flensberg et al., Phys. Rev. X **6**, 031016 (2016).

[22] T. Karzig, C. Knapp, R. M. Lutchyn, P. Bonderson, M. B. Hastings, C. Nayak, J. Alicea, K. Flensberg, S. Plugge, Y. Oreg et al., Phys. Rev. B **95**, 235305 (2017).

[23] F. Hassler and D. Schuricht, New J. Phys. **14**, 125018 (2012).

[24] A. Chew, A. Essin, and J. Alicea, Phys. Rev. B **96**, 121119 (2017).

[25] K. K. Likharev and A. B. Zorin, J. Low Temp. Phys. **59**, 347 (1985).

[26] D. V. Averin, A. B. Zorin, and K. K. Likharev, Zh. Eksp. Teor. Fiz. **88**, 692 (1985) [Sov. Phys. JETP **61**, 407 (1985)].

[27] S. V. Panyukov and A. D. Zaikin, J. Low Temp. Phys. **73**, 1 (1988).

[28] G. Schön and A. Zaikin, Phys. Rep. **198**, 237 (1990).

[29] H.-J. Kwon, K. Sengupta, and V. M. Yakovenko, Eur. Phys. J. B **37**, 349 (2004).

[30] L. Fu and C. L. Kane, Phys. Rev. B **79**, 161408 (2009).

[31] H.-J. Kwon, V. M. Yakovenko, and K. Sengupta, Low Temp. Phys. **30**, 613 (2004).

[32] D. M. Badiane, L. I. Glazman, M. Houzet, and J. S. Meyer, C. R. Phys. **14**, 840 (2013).

[33] D. Pekker, C.-Y. Hou, D. L. Bergman, S. Goldberg, İ. Adagideli, and F. Hassler, Phys. Rev. B **87**, 064506 (2013).

[34] Z.-T. Zhang, Z.-Y. Xue, and Y. Yu, Europhys. Lett. **118**, 57005 (2017).

[35] P. Matthews, P. Ribeiro, and A. M. García-García, Phys. Rev. Lett. **112**, 247001 (2014).

[36] C. Kurter, A. D. K. Finck, Y. S. Hor, and D. J. Van Harlingen, Nat. Commun. **6**, 7130 (2015).

[37] J. Wiedenmann, E. Bocquillon, R. S. Deacon, S. Hartinger, O. Herrmann, T. M. Klapwijk, L. Maier, C. Ames, C. Brüne, C. Gould *et al.*, Nat. Commun. **7**, 10303 (2016).

[38] G. Rastelli, Phys. Rev. A **86**, 012106 (2012).

[39] V. Bouchiat, D. Vion, P. Joyez, D. Esteve, and M. H. Devoret, Phys. Scr. **176**, 165 (1998).

[40] Y. Makhlin, G. Schön, and A. Shnirman, Rev. Mod. Phys. **73**, 357 (2001).

[41] D. Vion, A. Aassime, A. Cottet, P. Joyez, H. Pothier, C. Urbina, D. Esteve, and M. H. Devoret, Science **296**, 886 (2002).

[42] J. Koch, T. M. Yu, J. Gambetta, A. A. Houck, D. I. Schuster, J. Majer, A. Blais, M. H. Devoret, S. M. Girvin, and R. J. Schoelkopf, Phys. Rev. A **76**, 042319 (2007).

[43] S. M. Girvin, *Circuit QED: Superconducting Qubits Coupled to Microwave Photons* (Oxford University Press, Oxford, 2014), Chap. 3.

[44] H. Kleinert, *Tunneling*, 3rd ed. (World Scientific, Singapore, 2013), Chap. 17, pp. 1103–1202.

[45] H. J. W. Müller-Kirsten, *Path Integrals and Periodic Classical Configurations*, 2nd ed. (World Scientific, Singapore, 2013), Chap. 26, pp. 783–822.

[46] J. Ulrich, İ. Adagideli, D. Schuricht, and F. Hassler, Phys. Rev. B **90**, 075408 (2014).

[47] G. Mussardo, V. Riva, and G. Sotkov, Nucl. Phys. B **687**, 189 (2004).

[48] K. M. Leung, Phys. Rev. B **26**, 226 (1982).

[49] J. Singh, *The Tunneling Problem* (Wiley-VCH Verlag GmbH, Weinheim, Germany, 2007), pp. 126–169.

[50] C. R. Willis, M. El-Batanouny, S. Burdick, R. Boesch, and P. Sodano, Phys. Rev. B **35**, 3496 (1987).

[51] C. R. Willis, M. El-Batanouny, R. Boesch, and P. Sodano, Phys. Rev. B **40**, 686 (1989).

[52] A. J. Leggett, S. Chakravarty, A. T. Dorsey, M. P. A. Fisher, A. Garg, and W. Zwerger, Rev. Mod. Phys. **59**, 1 (1987).